UNIVERSITY OF BIRMINGHAM

Tunable millimetre-wave phase shifting surfaces using piezoelectric actuators

Mavridou, Marina; Feresidis, Alexandros; Gardner, Peter; Hall, Peter

[Link to publication on Research at Birmingham portal](#)

Tunable Millimetre-wave Phase Shifting Surfaces Using Piezoelectric Actuators

M. Mavridou, A. P. Feresidis, P. Gardner and P. S. Hall

School of Electronic, Electrical and Computer Engineering,
University of Birmingham,
Birmingham, B15 2TT, UK
email: a.feresidis@bham.ac.uk

Abstract

A novel technique for tuning periodic phase shifting surfaces at millimetre-waves is presented. The proposed structure consists of a periodic surface placed over a ground plane creating an air cavity. The periodic surface is formed by a two dimensional array of metallic square loop elements printed on a 0.8mm thick dielectric substrate. When excited by a plane wave, the structure is acting as an artificial impedance surface, reflecting the incident wave with a wide range of phase values within a specific frequency band. The tuning is achieved by means of a small number of piezoelectric actuators which support the periodic surface. The actuators are placed around the periodic surfaces thereby not interfering with the radiation performance and introducing no losses. They produce a displacement between the periodic surface and the ground plane when voltage is applied, which in turn changes the reflection phase response of the structure. Full wave periodic simulations have been carried out in 3D electromagnetic simulation software (CST Microwave Studio^{TM}) to extract the reflection characteristics and evaluate the expected tuning range of the proposed structure. A prototype has been fabricated and measured validating the concept.

Index Terms Artificial impedance surfaces, Periodic surfaces, Frequency Selective Surfaces, Spatial phase shifters, Reconfigurable antennas, Tunable antennas

1. INTRODUCTION

Periodic surfaces consist of arrays of metallic elements printed on a dielectric substrate or apertures in a conducting screen. When placed at close proximity to a ground plane, for example metallic elements printed on a grounded dielectric substrate, they reflect incident waves with a zero degrees phase shift and are termed High Impedance Surfaces (HIS) or Artificial Magnetic Conductors (AMC). As such they can be applied as ground planes in printed antennas [1] or in cavity antennas to reduce their profile [2, 3]. Furthermore, doubly periodic arrays placed over a ground plane have also been employed for their phase shifting properties in numerous applications, where they are operated at various reflection phase values and not just at zero degrees. Such applications include reflectarrays [4], compact waveguides [5], subwavelength-profile resonant cavity leaky-wave antennas [6] and anisotropic polarisation converters [7].

Tuning the response of periodic surfaces has attracted significant interest in the last few years. The frequency response of such a surface depends on the periodicity, the size and shape of the elements, and the thickness and electromagnetic properties of the supporting material. Various techniques have been employed to dynamically change one of the above characteristics in order to obtain a tunable periodic surface. At lower microwave frequencies one of the available techniques for electronic tuning is the use of varactor or PIN diodes [8-10], but their use can be prohibitive at higher mm-wave frequencies due to losses and parasitic effects. In [11] a mechanically tunable high impedance surface has been proposed performing as a reflector for reconfigurable beam steering at frequencies around 2.5GHz. Micro-Electro-Mechanical Systems (MEMS) have been employed at lower mm-wave frequencies to achieve tuning of periodic surfaces by means of appropriate integrated micro –

actuators that mechanically change the effective size and/or orientation of the array's elements and have shown promising results [12]. Finally, tunable materials have been studied, such as ferroelectrics at lower microwave frequencies [13, 14] and more recently liquid crystals [15- 17], at higher mm-wave. Liquid crystal materials have produced promising results particularly for submm-wave frequencies, but with several constraints in terms of the losses and very low tuning speeds [17].

In this paper, a new technique for tuning the response of a grounded periodic phase shifting surface is presented for operation at approximately 60GHz. The periodic surface consists of an array of metallic square loop elements printed on a dielectric substrate. The surface is placed over a ground plane creating an air cavity and providing a range of reflection phase values. The tuning is achieved by means of piezoelectric actuators which support the surface and produce a displacement under a DC bias, thus changing the cavity thickness. The reflection phase response of the structure is strongly dependant on the cavity thickness, which leads to a significant tuning range. A major advantage of the proposed design is that the actuators are placed around the periodic surfaces thereby not interfering with their radiation performance and introducing no losses to the overall structure which is particularly important for higher frequencies. Moreover, the technique is scalable to higher mm-wave and even submm-wave frequencies,

2. **Design of Tunable Periodic Surface**

The proposed structure is shown in Fig. 1(a). A square loop metallic patch has been chosen as the unit cell of the periodic surface printed on a 0.8mm thick TLY-5 dielectric substrate (ε_r=2.2, tanδ=0.0009). The periodicity and the patch dimensions are shown in Fig. 1(b). The surface is placed over a ground plane forming an air cavity (Fig. 1(a, c)) at a distance t. A

plastic base is used to support the ground plane and the piezo-actuators, which in turn support the periodic surface.
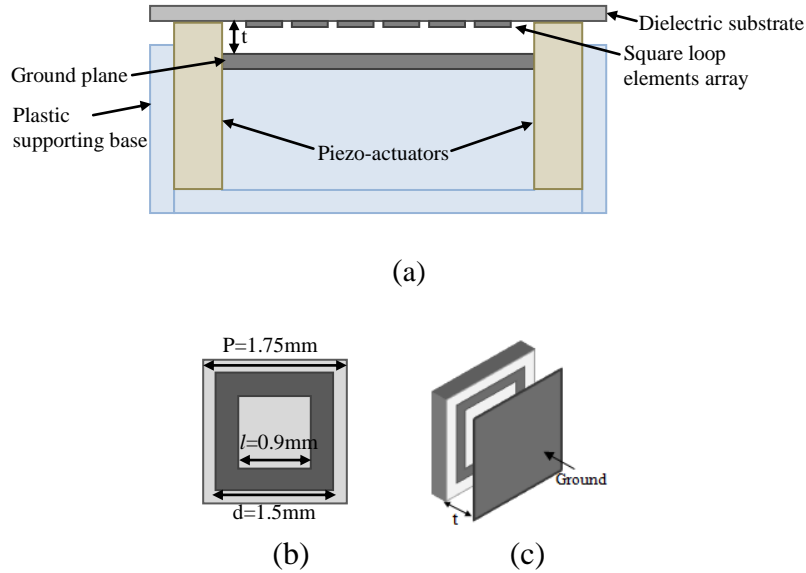

(a)

(b)   (c)

Figure 1: (a) Cross section of the complete structure (dimensions are not to scale), (b) Front view of the unit cell, (c) Perspective of the unit cell placed at distance t from the ground plane

2.1   Tuning Range study

Full wave analysis has been carried out in CST to extract the reflection characteristics of the unit cell and periodic boundary conditions have been employed which assume an infinite structure. The cavity thickness was initially set at t=50μm which produced the first cavity resonance just below 60GHz. The magnitude of the reflection coefficient is shown in Fig. 2(a) showing how the cavity resonance is tuned by changing the cavity thickness. It should be noted that a minimum occurs at the frequency of the cavity resonance. However, the periodic surface design proposed here is based on closely spaced subwavelength (less than λ/3) square loop elements which yield low losses. The simulated phase of the reflection coefficient is shown in Fig. 2(b) for different cavity thicknesses which correspond to a displacement Δt from zero to 20μm. It can be observed that a significant phase shift is obtained with this design ($\Delta\varphi \approx 120^{o}$ for Δt=20μm). However positioning and aligning the periodic surface at

4

such a small distance from the ground plane proved to be non trivial for our first experiment as described in section 4, therefore for practical reasons the cavity thickness was changed to t=2.5mm. In this case a maximum slope of the reflection phase at about 62GHz has been achieved. This is the second resonance of the cavity with that particular thickness while the first resonance occurs at about 10GHz. In the case of the new cavity, for a displacement of Δt =10μm and Δt=20μm, a phase shift of 90° and 126° has been obtained respectively for operation at 61.8GHz which is approximately the frequency of the inflection point (i.e. maximum slope) of the phase curves (Fig. 3). Furthermore, the reflection magnitude is higher, i.e. the losses are smaller, compared to the initial cavity thickness, which is a useful feature for our design. This is due to the lower currents induced on the elements of the periodic surface for increased cavity thickness, as has been observed in simulations. It should be noted that the reflection phase in both cases is not 0° at the cavity resonance, but ~ -150°. This is because of the additional phase shift that occurs in the dielectric substrate of the periodic surface which can be easily calculated from the optical path length.

Different geometries have been considered for the proposed configuration and square loop metallic patch has been chosen based on the fast variation of its reflection phase with the frequency. This characteristic is the key aspect of the design in order to make it more sensitive to small variations of the cavity thickness and achieve a large phase shift. In Fig. 4 the reflection phase for the proposed square loop unit cell and a simple square patch with the same periodicity and edge 1.5mm are shown for comparison. It is evident that the slope for the square patch has a smaller gradient, which results in a smaller phase shift for the same variation of the cavity thickness. This is in line with the variations of the reflection characteristics of free-standing Frequency Selective Surfaces (FSSs) which another term that can be used to describe this type of periodic surfaces [18]
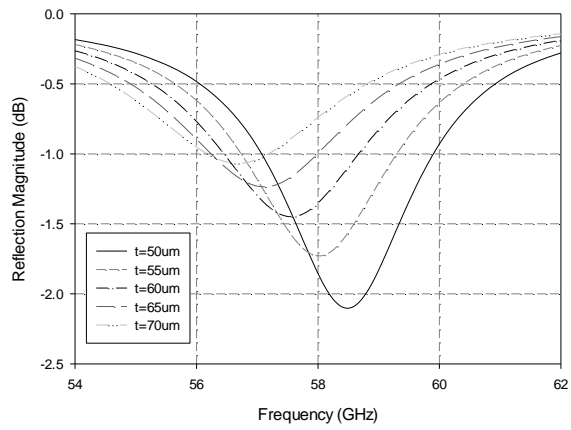
(a)
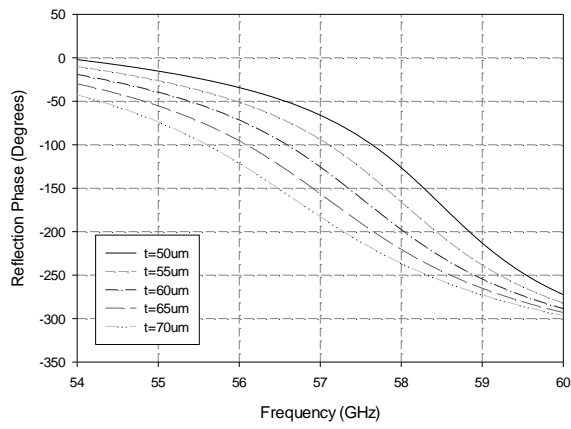
(b)

Figure 2: (a) Reflection magnitude and (b) Reflection phase for t=50um+Δt

(a)

(b)
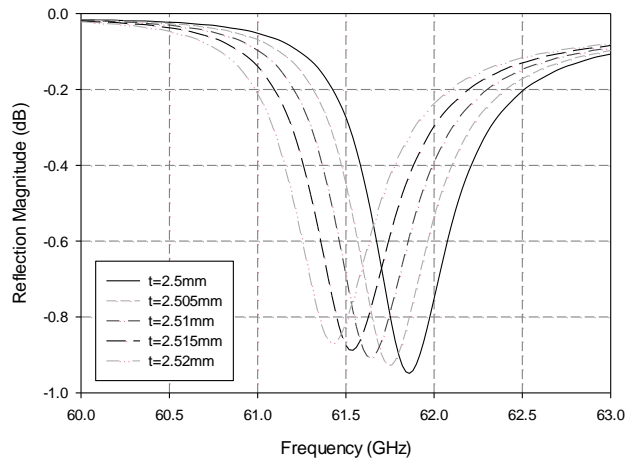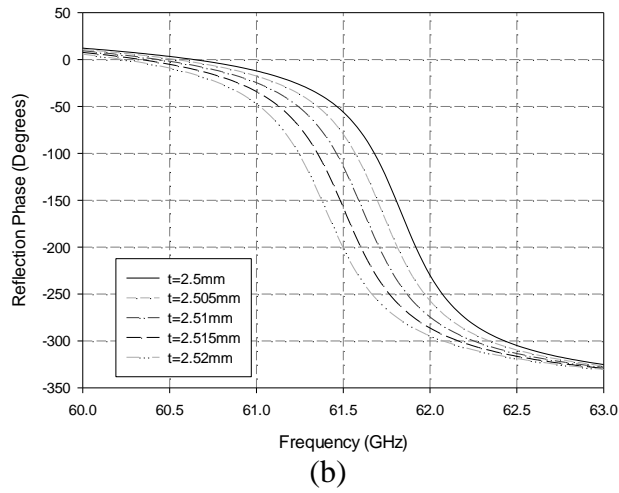
Figure 3: (a) Reflection magnitude and (b) Reflection phase for t=2.5mm+Δt
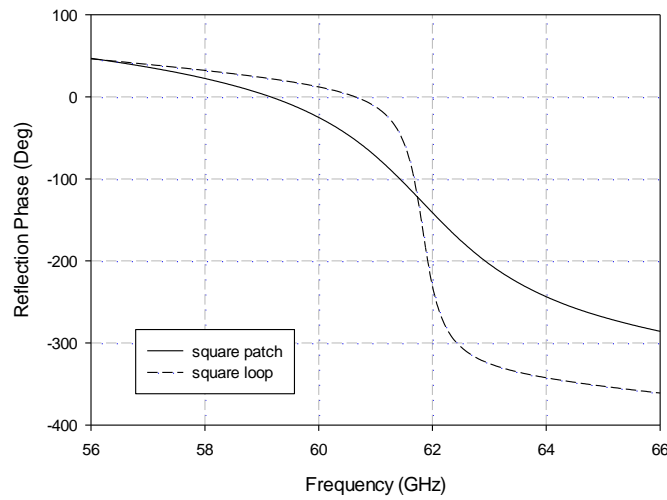
Figure 4: Reflection phase comparison for a square patch array and the proposed square

loop design

2.2   Losses Evaluation

In this section an investigation is being carried out on the main factors contributing to the losses in the proposed configuration and on whether a more appropriate design could have been chosen instead, exhibiting less loss.

Initially, simulations have been carried out for the unit cell of the structure for three different cases. First, taking into account both dielectric and metal losses, then only dielectric losses with lossless metal and finally only metal losses with the dielectric considered lossless. The magnitude of the reflection coefficient for all three cases is depicted in Fig. 5. It can be observed that the minimum for lossy materials is -0.95dB while for lossy dielectric only and lossy metal only it is 0.07dB and 0.88dB respectively. This means the losses are mainly attributed to the metal with only a very small part related to the dielectric substrate.

Subsequently, another study has been carried out to evaluate the losses for two other possible configurations. The first case that has been considered comes from placing the periodic surface upside-down, so that the array is on top and the AMC cavity is formed partly from the dielectric substrate and partly from air. In order to achieve a resonance at the same frequency the air cavity was set at 1.382mm. In this case the minimum of the reflection magnitude is -1.8dB as opposed to -0.95dB which corresponds to the original configuration. Furthermore, a dielectric filled cavity was also simulated with the cavity thickness now set at 1.694mm. The dielectric that has been employed is the same one used for the original configuration i.e. TLY-5 with dielectric constant ε_r=2.2 and tanδ=0.0009. The minimum in this case is equal to -2.4dB. The reflection coefficient magnitude for all the aforementioned configurations is presented in Fig. 6. It is evident that the proposed design is greatly advantageous in terms of losses compared with the two other configurations.
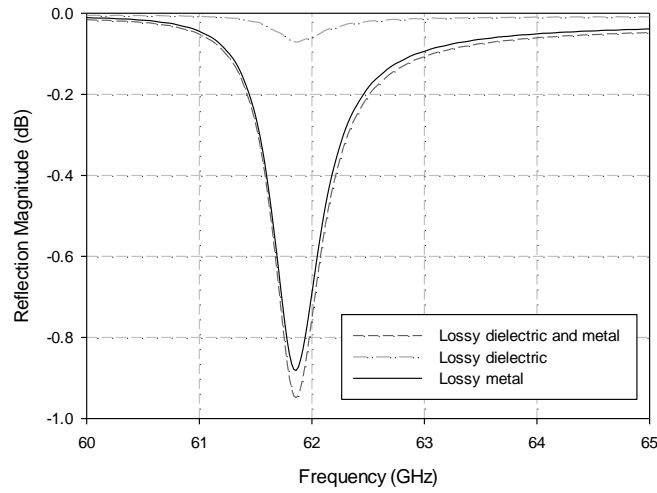
Figure 5: Magnitude of the reflection coefficient for lossy and lossless materials
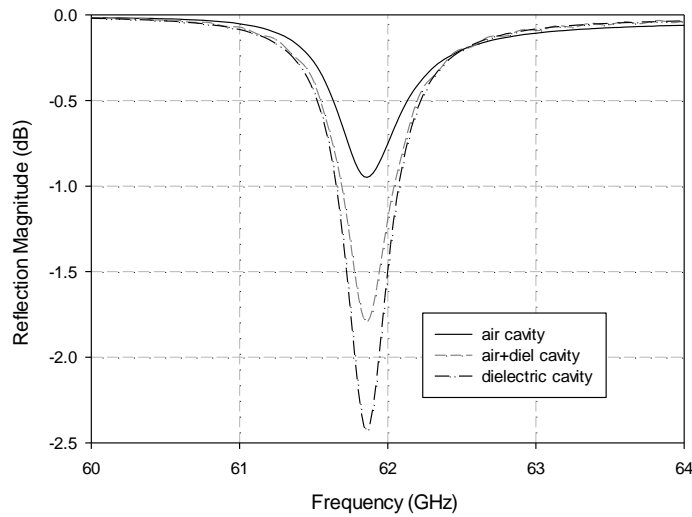
Figure 6: Magnitude of the reflection coefficient for different type of cavities

3. Piezoelectric Actuators

As mentioned in the introduction two piezoelectric actuators are employed to support the periodic surface as shown in Fig. 1(a) and produce a tunable reflection phase shift by dynamically changing the air cavity thickness. The simulation results presented in the previous section were obtained by parametrically changing the cavity thickness to model the

9

displacement obtained from the piezoelectric actuators. In this section the operation of this type of actuators is described.

The principle of operation of the piezo-actuators is based on the inverse piezoelectric phenomenon. They are built from Lead (Pb) Zirconate (Zr) Titanate (Ti) (PZT) ceramic disks placed on top of each other forming stacks. A schematic diagram can be seen in Fig. 7(a). Due to the inverse piezoelectric phenomenon, each of the disks has the property of expanding vertically when exposed to an electric potential. In the stack, the disks are separated by thin metallic electrodes where the voltage is applied. Consequently, the total expansion ΔL of the actuator is the sum of the expansion of each disk. The maximum operating voltage is proportional to the thickness of the disks and the total displacement a piezo-stack actuator can produce is proportional to its total length and more specifically equal to 10% of its length. An estimation of the displacement can be made from (1) where d_{33} is a strain coefficient that describes the forces applied to the actuator and the properties of the piezoelectric material used, n is the number of ceramic layers and V is the applied voltage [16].

$$\Delta L \approx d_{33} \cdot n \cdot V \qquad (1)$$

For the proposed design two commercial actuators, P-885.51 from Physik Intrumente (PI), are used. The photograph in Fig. 7(b) shows one of the actuators without the wires used to apply the DC voltage which are carefully soldered to one of the small metallic bits visible in the picture. The "+" sign indicates the positive polarization. This particular model is 18mm long and can achieve a maximum displacement of 18μm for an applied voltage of 120V. This is satisfactory for the requirements of the proposed structure, as shown from the simulation results. Nevertheless, in order to achieve maximum displacement a mechanical preloading for the actuators is desired, for example a spring that should be placed between the actuator and

10

Therefore without preloading, a slightly less displacement is expected.

The main advantages of these piezoelectric actuators are their high accuracy and reliability for nano-positioning applications, their low-cost and very fast response in the order of microseconds, which is important for applications such as communication and radar systems. Moreover, they exhibit sub-nanometer resolution, high energy conversion efficiency, low voltage operation, large force and no Electromagnetic Interference (EMI) [16].
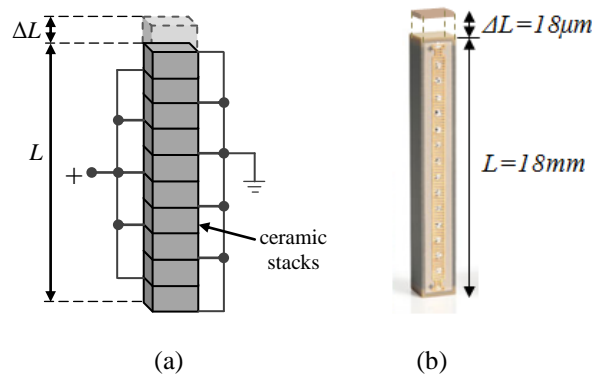

(a)   (b)

Figure 7: Piezoelectric actuator (a) schematic diagram, (b) commercial actuator P-885.51

from PI

A characterization of the two actuators has been carried out to validate their expansion properties and also to test the operation of the biasing and their integration in the plastic base used for supporting the structure. An optical interferometer has been used in order to be able to measure the displacement which is in the order of micrometers. The displacement of both actuators for voltages from 0 to 120V has been measured and the results are presented in Table I. As it can be observed from the table each actuator achieved different displacement for the same applied voltage. For voltage values up to 20V no measurable displacement occurred while the maximum ΔL was 14.3μm and 10.5 μm for actuators 1 and 2 respectively.

Although a slight difference was expected between them, the fact that actuator 2 achieved less displacement, is attributed to the way the negative electrode has been soldered on it. As can be seen from Fig. 8(b), there is excessive soldering on the left actuator (actuator 2) that may prevent the proper expansion of the ceramic disk that lies in the specific position. Furthermore, it should be noted that there was no preloading used with the actuators which justifies why they have not reached the nominal maximum ΔL (18μm).

TABLE I

PIEZO-ACTUATORS DISPLACEMENT MEASUREMENT FOR DC VOLTAGES FROM 30 TO 120V

DC Voltage (V)	Actuator 1 ΔL (μm)	Actuator 2 ΔL (μm)
30	1.6	0.7
40	3.5	0.9
50	4.5	1.4
60	6	2.9
70	7.4	3.7
80	8.5	4.1
90	10.8	5.5
100	11.8	8.5
110	12.9	9.1
120	14.3	10.5

4. Fabrication and Measurements

A prototype of the proposed design has been fabricated and measured to validate the simulation results. Initially, a 23x23 (8λx8λ) square loop element array printed on a 60x60mm^2 TLY-5 dielectric substrate has been fabricated as shown in Fig. 8(a). In order to support the actuators and the ground plane a plastic base has been made. It was designed so that the two actuators would exactly fit on each side of a plane surface where the ground plane (40x60mm^2) is mounted. The starting position of the actuators is adjustable with screws to achieve the desired cavity thickness which in this case is 2.5mm. Finally, the periodic surface

has been secured on top of the two actuators. A photograph of the complete structure is shown in Fig. 8(b).
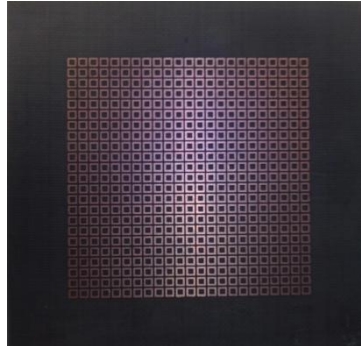
(a)

(b)

Figure 8: (a) Photograph of fabricated 23x23 element array (b) Photograph of the structure

Once the structure was complete, two standard gain V-band horn antennas were employed in order to measure the magnitude and phase of the reflection coefficient from the periodic surface. Both antennas were fed from a Vector Network Analyzer (VNA). One was connected to channel 1 and served as the transmitter and the other was connected to channel 2 and served as the receiver. Before starting the measurement, a full two-port calibration of the VNA was carried out for the frequency range of interest. The horns were positioned aiming towards the periodic surface at a distance of more than 20cm away from it and at an angle of incidence/reflection of about 15°. The reflection has been measured through the S21 between the two horn antennas for different applied voltage at the actuators. The phase response for

voltages 0V, 60V and 120V is presented in Fig. 9 after being normalized with respect to a measurement of a flat metallic surface placed in the same position as the array. It can be seen that a phase shift of about 30° is obtained at about 58.2 GHz when 120V are applied to the piezo-actuators with respect to the unbiased state.
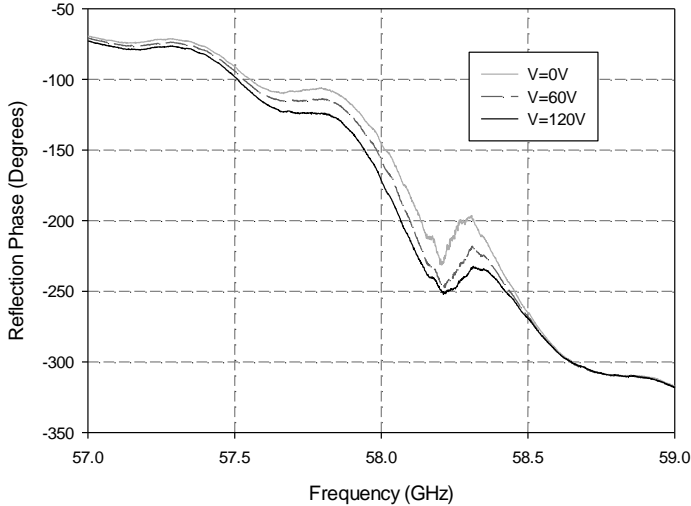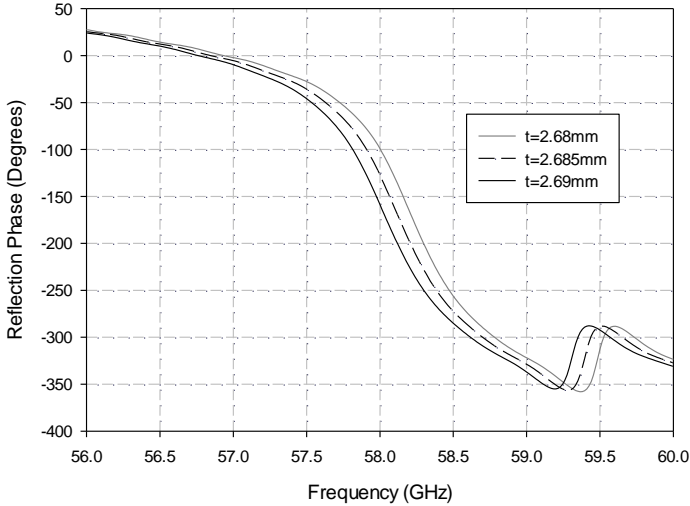

Figure 9: Measured reflection phase of the fabricated prototype for three different voltages

Although the concept of the design, which was to obtain a dynamic phase shifting surface, has been validated, there is a disagreement with the simulation results. In particular, the obtained phase shift is less than what was expected from the periodic simulations. The disagreement

14

can be attributed to two major factors. First, the most important factor for this discrepancy is the finite size of the measured periodic surface. Indeed, we have carried out a full wave simulation of a finite size structure in CST, and it was found that the phase shift for $\Delta t=10\mu m$ is about 60° which is closer to the measured one than the infinite size simulation result. The finite structure simulation also produced the sharp peak that appears in the measurements just above the cavity resonance (over 58.3GHz). Inspection of the electric field inside the cavity showed that this effect is due to a resonance across the lateral dimensions of the finite array which distorts the field distribution in this direction. Second, the disagreement can also be attributed to the imperfect flatness of the two surfaces and the approximate alignment between them which is particularly crucial at mm-wave frequencies and should ideally be performed using quasi-optical techniques. Finally, the measured frequency of the cavity resonance (where the slope in the phase is maximum) is 58.2GHz while the simulated one is 61.8GHz. This is because the actual cavity thickness was slightly more than 2.5mm which resulted in a resonance at a lower frequency.

5. Conclusion

A tunable mm-wave phase shifting surface has been presented using piezoelectric actuators to achieve the dynamic tuning of the reflection phase. The proposed structure consists of an air cavity created between a square loop element periodic surface and a ground plane. Two piezoelectric actuators are employed to support the periodic surface. The concept is based on the displacement produced by the actuators under DC bias, which changes the cavity thickness and results in a significant tuning of the reflection phase response for operation around 60GHz. A study of the losses has been also carried out. Finally a prototype has been fabricated and measured validating the proposed design.

6. Acknowledgment

7. References

[1] Sievenpiper, D., Lijun, Z., Broas, R. F., Alexopoulos, N. G., Yablonovitch, E.: 'High-impedance electromagnetic surfaces with a forbidden frequency band', IEEE Trans Microw. Theory Tech., 1999, 47, (11), pp. 2059-2074

[2] Wang, S., Feresidis, A., Goussetis, G., Vardaxoglou, J. C.: 'Low profile resonant cavity antenna with artificial magnetic conductor ground plane', Electron. Lett., 2004, 40, (7), pp. 405-406

[3] Feresidis, A. P., Goussetis, G., Wang, S., Vardaxoglou, J. C.: 'Artificial magnetic conductor surfaces and their application to low profile high gain planar antennas', IEEE Trans. Antennas Propag., Special Issue on AMC, Soft Hard Surfaces and Other Complex Surfaces, 2005, 53, (1), pp. 209-215

[4] Huang, J., and Encinar, J.A.: 'Reflectarray antennas', (John Wiley, Hoboken, NJ, 2008)

[5] Maci, S., Caiazzo, M., Cucini, A., Casaletti, M.: 'A pole-zeromatching method for EBG surfaces composed of a dipole FSS printed on a grounded dielectric slab', IEEE Trans. Antennas Propag., 2005, 53, (1), pp. 70–81

[6] Kelly, J. R., Kokkinos, T., Feresidis, A. P.: 'Analysis and design of sub-wavelength resonant cavity type 2-D leaky-wave antennas', IEEE Trans. Antennas Propag., 2008, 56, (9), pp. 2817–2825

[7] Doumanis, E., Goussetis, G., Gomez-Tornero, J.-L., Cahill, R., Fusco, V.: 'Anisotropic impedance surfaces for linear to circular polarization', IEEE Trans. Antennas Propag., 2012, 60, (1), pp. 212–219

[8] Costa, F., Monorchio, A., Talarico, S., Valeri, F.M.: 'An Active High-Impedance Surface for Low-Profile Tunable and Steerable Antennas', Antennas and Wireless Propagation Letters, IEEE, 2008, 7, pp. 676-680

[9] Weily, A. R., Bird, T. S., Guo, Y. J.: 'A reconfigurable high-gain partially reflecting surface antenna', IEEE Trans. Antennas Propag., 2008, 56, (11), pp. 3382–3390

[10] Guzmán-Quirós, R., Gómez-Tornero, J.L., Weily, A.R., Guo, Y.J.: 'Electronically steerable 1-D Fabry-Pérot leaky-wave antenna employing a tunable high impedance surface', IEEE Trans. Antennas Propag., 2012, 60, (11), pp.5046-5055

[11] Sievenpiper, D., Schaffner, J., Loo, R., Tangonan, G., Ontiveros, S., Harold, R.: 'A tunable impedance surface performing as a reconfigurable beam steering reflector', IEEE Trans. Antennas Propag., 2002, 50, (3), pp. 384–390

[12] Gianvittorio, J. P., Zendejas, J. M., Rahmat-Samii, Y., Judy, J. W.: 'Reconfigurable MEMS-enabled frequency selective surfaces', Electronics Letters, 2002, 38, (25), pp.1627-1628

[13] Parker, E. A., Savia, S. B.: 'Active frequency selective surfaces with ferroelectric substrates', *Proc. Inst. Elect. Eng. Microwaves, Antennas and Propagation*, 2001, 148, pp. 103–108

[14] Lovat, G., Burghignoli, P., Celozzi, S.: 'A tunable ferroelectric antenna for fixed-frequency scanning applications', IEEE Antennas Wireless Propag. Lett., 2006, 5, pp. 353–356

[15] Hu, W., Dickie, R., Cahill, R., *et al.*: 'Liquid crystal tunable mm wave frequency selective surface', IEEE Microw. Wireless Compon. Lett., 2007, 17, (9), pp. 667–700

[16] Hu, W., Ismail, M.Y., Cahill, R., *et al.*: 'Liquid-crystal-based reflectarray antenna with electronically switchable monopulse patterns', Electronics Letters , 2007, 43, (14)

[17] Perez-Palomino, G., Baine, P., Dickie, R., *et al.*: 'Design and Experimental Validation of Liquid Crystal-Based Reconfigurable Reflectarray Elements With Improved Bandwidth in F-Band', *Antennas and Propagation, IEEE Transactions on*, 2013, 61, (4), pp.1704-1713

[18] Munk, B.A.: 'Frequency selective surfaces, theory and design' (John Wiley & Sons Inc., New York, 2000)

[19] www.physikinstrumente.co.uk